



# Selective hydroxylation of cyclohexene over Fe-bipyridine complexes encapsulated into Y-type zeolite under environment-friendly conditions

Syuhei Yamaguchi<sup>a</sup>, Tomohiro Fukura<sup>a</sup>, Keiko Takiguchi<sup>a</sup>, Chiharu Fujita<sup>a</sup>, Maiko Nishibori<sup>b</sup>, Yasutake Teraoka<sup>b</sup>, Hidenori Yahiro<sup>a,\*</sup>

<sup>a</sup> Department of Materials Science and Biotechnology, Graduate School of Science and Engineering, Ehime University, Matsuyama 790-8577, Japan

<sup>b</sup> Department of Energy and Material Sciences, Faculty of Engineering Sciences, Kyushu University, Kasuga, Fukuoka 816-8580, Japan

## ARTICLE INFO

### Article history:

Received 29 April 2014

Received in revised form 16 July 2014

Accepted 18 July 2014

Available online xxx

### Keywords:

Fe complex

Zeolite

Hydroxylation

Hydrogen peroxide

Molecular oxygen

## ABSTRACT

Fe-bipyridine complexes encapsulated into Na-Y ( $[Fe(bpy)_3]^{2+}@\text{Y}$ ) were prepared and their catalytic activities for oxidation of cyclohexene with hydrogen peroxide in  $\text{CH}_3\text{CN}$  and  $\text{H}_2\text{O}$  solvents were investigated. The prepared  $[Fe(bpy)_3]^{2+}@\text{Y}$  was characterized by several methods and it was found that slightly distorted or compressed  $[Fe(bpy)_3]^{2+}$  ions were formed within supercages of Y-type zeolite.  $[Fe(bpy)_3]^{2+}@\text{Y}$  catalyst exhibited both higher activity and higher selectivity to 2-cyclohexen-1-ol in water solvent than another Fe catalysts. In addition, the selective hydroxylation of cyclohexene to 2-cyclohexen-1-ol with molecular oxygen was successfully achieved for  $[Fe(bpy)_3]^{2+}@\text{Y}$  catalyst.

© 2014 Elsevier B.V. All rights reserved.

## 1. Introduction

From the view point of solution to environmental problems, the development of green chemistry procedures and environmental friendly technologies is the important subject to keep sustainable growth. One of the most interesting areas in catalysis is the development of inorganic–organic hybrid materials for catalytic oxidation reactions [1–3]. The ability of mononuclear non-heme iron hydroxylases to catalyze the activation of C–H bonds by molecular oxygen ( $\text{O}_2$ ) has inspired many synthetic chemists to explore functional small molecule mimics of these enzymes [4,5]. The catalysis of mononuclear iron using hydrogen peroxide ( $\text{H}_2\text{O}_2$ ) instead of  $\text{O}_2$  as a terminal oxidant for alkane oxidation has been investigated [4,5]. A few examples of iron-catalyzed hydrocarbon oxidation by  $\text{O}_2$  have been proposed and required either a sacrificial reductant [6,7] or a weak C–H bond on the substrate [8–12]. Many researchers have reported that cyclohexene oxide and cyclohexane diol were formed by the oxidation of cyclohexene with  $\text{H}_2\text{O}_2$  using Fe complexes controlled by designed tetradentate ligands [4,13–15]. However, little

is known about the selective hydroxylation of cyclohexene with  $\text{H}_2\text{O}_2$  using Fe complexes to 2-cyclohexen-1-ol, due to the subsequent oxidation of 2-cyclohexen-1-ol to 1-one [15]. In recent years, the immobilization of transition metal complexes on the surface of supports or the encapsulation of the transition metal complexes inside porous materials has received considerable attention. Such an application results in a significant enhancement of novel catalytic activities that homogeneous catalysts have not exhibited yet [16–18]. Utilizing water as an alternate to toxic and harmful organic synthesis has been extensively studied [19–24]. Thus, the combination of catalysts with iron as a ubiquitous metal and water as a solvent is very attractive from a viewpoint of green sustainable chemistry [25–28].

The Y-type zeolite belonging to the faujasite family has large cavities, so-called supercages, with a diameter of ca. 13.0 Å [29]. The supercages are connected to each other by tunnels or windows with a widest diameter of ca. 7.4 Å. The estimated kinetic diameter of  $[Fe(bpy)_3]^{2+}$  complex (ca. 12 Å) is larger than a window size of supercage so that the  $[Fe(bpy)_3]^{2+}$  complex synthesized in supercage cannot go out from the cavity. Therefore,  $[Fe(bpy)_3]^{2+}$  complexes encapsulated into Na-Y ( $[Fe(bpy)_3]^{2+}@\text{Y}$ ) have been utilized as a heterogeneous oxidation catalyst [2,30–33]. However there is less information about the activity of  $[Fe(bpy)_3]^{2+}@\text{Y}$  catalyst for selective oxidation in water solvent [34]. In this report,

\* Corresponding author. Tel.: +81 89 927 9929; fax: +81 89 927 9946.

E-mail address: [hyahiro@ehime-u.ac.jp](mailto:hyahiro@ehime-u.ac.jp) (H. Yahiro).

$[\text{Fe}(\text{bpy})_3]^{2+}@\text{Y}$  was characterized by several methods and its catalytic activity for oxidation of cyclohexene with  $\text{H}_2\text{O}_2$  and  $\text{O}_2$  was investigated in  $\text{CH}_3\text{CN}$  and  $\text{H}_2\text{O}$  solvents.

## 2. Experimental

### 2.1. Materials and instruments

Na ion-exchanged Y-type zeolite (Na-Y) with  $\text{SiO}_2/\text{Al}_2\text{O}_3 = 5.5$  was supplied from Tosoh Co. All chemicals,  $\text{FeSO}_4 \cdot 7\text{H}_2\text{O}$  (Wako, >99%), 2,2'-bipyridine (Wako, 99.5%), methanol (Wako, 99.8%), cyclohexene (Wako, 97.0%), 30% aqueous hydrogen peroxide (Wako, 30–35.5%), cyclohexene oxide (TCL, >98%), 2-cyclohexen-1-ol (Aldrich, 95%), 2-cyclohexen-1-one (Wako, 95%), mixture of cis and trans-1,2-cyclohexan diols (Alfa Aesar), cis-1,2-cyclohexen diol (Wako), 1-octanol (Wako, 98.0%), and acetonitrile (Wako, 99.5%), were used as received. Cyclohexene was used as a substrate after purification with treatment of activated alumina and distillation to remove peroxide and oxidation species derived from cyclohexene.

The powder XRD patterns of catalysts were collected on a Rigaku MiniFlex II diffractometer using  $\text{CuK}\alpha$  radiation. UV-vis spectra were recorded on a Hitachi U-4000 spectrometer for solid samples or on Shimadzu U-1200 for liquid samples. GC analysis was performed on Shimadzu GC-14B with a flame ionization detector equipped with a Stabilwax capillary column (internal diameter = 0.25 mm, length = 30 m) at the nature of polar liquid phase. GC-MS spectra were recorded on Shimadzu GCMS-QP5050A (ionization voltage = 70 eV) equipped with a DB-1MS capillary column (internal diameter = 0.25 mm, length = 30 m) at the nature of non-polar liquid phase.

Fe K-edge X-ray Absorption Fine Structure (XAFS) spectra were measured at room temperature in transmission mode at Kyushu University Beamline (BL06) in the Kyushu Synchrotron Light Research Center (SAGA-LS), Tosa, Japan (proposal no. 2012IK009). Appropriate amount of powder samples and 80 mg of boron nitride powder were mixed and pressed into pellets of 10 mm in diameter. Synchrotron radiation was monochromated by a Si (111) double crystal and a cylindrical mirror coated by rhodium was used to eliminate higher harmonics. Extended X-ray absorption fine structure (EXAFS) data were analyzed using a data analysis program, REX2000.

### 2.2. Preparation of Fe-containing catalysts

#### 2.2.1. Preparation of $[\text{Fe}(\text{bpy})_3]^{2+}@\text{Y}$ catalyst

Na-Y zeolite (5.0 g) was ion-exchanged by a conventional method using aqueous solution (300 mL) of  $\text{FeSO}_4 \cdot 7\text{H}_2\text{O}$  (0.2 g, 0.72 mmol) to yield iron(II) ion-exchanged Y-type zeolite (Fe-Y) [35]. The prepared Fe-Y (1.0 g) was refluxed in an aqueous solution (100 mL) of 2,2'-bipyridine (bpy) (0.47 g, 3.0 mmol) for 20 h, followed by filtration, washing with water and methanol by Soxhlet extractor, and drying at room temperature under vacuum to give  $[\text{Fe}(\text{bpy})_3]^{2+}@\text{Y}$  as a reddish-pink powder.

Reddish-pink power ( $[\text{Fe}(\text{bpy})_3]^{2+}@\text{Y}$ ): elemental analyses. C, 5.12; H, 1.99; N, 1.22; Na, 5.38; Fe, 0.88; and Al, 8.08 wt%.

#### 2.2.2. Preparation of $[\text{Fe}(\text{bpy})_3](\text{ClO}_4)_2$ as a control catalyst for $[\text{Fe}(\text{bpy})_3]^{2+}@\text{Y}$

The complex  $[\text{Fe}(\text{bpy})_3](\text{ClO}_4)_2$  for comparison with  $[\text{Fe}(\text{bpy})_3]^{2+}@\text{Y}$  was synthesized as described in previous work [36]. 2,2'-Bipyridine (0.78 g, 5.0 mmol) was added into  $\text{H}_2\text{O}$  solution (100 mL) of  $\text{FeSO}_4 \cdot 7\text{H}_2\text{O}$  (0.42 g, 1.5 mmol) at about 60 °C and stirred at the same temperature for 1 h. After the addition of sodium perchlorate (0.85 g, 7.0 mmol) into the mixture solution, a reddish precipitate formed immediately. After filtration, recrystallization

**Table 1**

Experimental and theoretical values of Fe content, C/N and Fe/bpy in  $[\text{Fe}(\text{bpy})_3]^{2+}@\text{Y}$ .

	Fe content/wt% <sup>a</sup>	C/N <sup>b</sup>	Fe/bpy molar ratio
Experimental	0.88	4.9	Fe:bpy = 1.0:2.8
Theoretical	–	5.0	Fe:bpy = 1.0:3.0

<sup>a</sup> ICP analysis results.

<sup>b</sup> CHN elemental analysis results.

of the precipitate from  $\text{CH}_3\text{CN}$ /diethylether gave needle-like red single crystals, suitable for X-ray structural analysis.

Needle-like reddish solid;  $\text{C}_{30}\text{H}_{24}\text{Cl}_2\text{FeN}_6\text{O}_8$  (723.30) calcd. C 49.82, H 3.34, N 11.62; found C 49.51, H 3.37, N 11.64.

### 2.3. Catalytic oxidation

The catalytic oxidations were carried out with a glass tube reactor. A typical procedure was as follows; catalyst (7.9  $\mu\text{mol}$ ), solvent ( $\text{MeCN}$  and/or  $\text{H}_2\text{O}$ ) (10 mL), and cyclohexene (7.9 mmol) were charged, and 30% aqueous hydrogen peroxide (0.8 mmol) was added in glass tube reactor under Ar or  $\text{O}_2$ . The reaction was carried out at 50 °C. After the reaction, triphenylphosphine as a quencher was charged, and 1-octanol as an internal standard was added in glass tube reactor. The reaction solution was analyzed by GC in combination with mass spectroscopy. The products were identified by the comparison of mass spectra with those authentic samples. GC-MS condition was as follows: interface temperature (150 °C), detector temperature (230 °C), oven temperature (85 °C (hold for 10 min) to 220 °C at 30 °C/min (hold for 5 min)), and retention times (2.5, 3.7, 4.0, 4.5, 8.3, 8.4, and 9.4 min for cyclohexene, cyclohexene oxide, 2-cyclohexen-1-ol, 2-cyclohexen-1-one, trans-1,2-cyclohexan diol, cis-1,2-cyclohexen diol, and 1-octanol (internal standard), respectively). The carbon balance (mass balance) in each experiment was in the range of 95–100%.

Similarly, the reaction solution was analyzed by GC-FID in order to confirm the presence or the absence of adipic acid as an oxidation product of cyclohexene. GC-FID condition was as follows: interface temperature (230 °C), detector temperature (250 °C), column temperature (150 °C (hold for 1 min) to 245 °C at 30 °C/min (hold for 20 min)), and retention times (1.23, 1.41, 1.80, 1.84, 1.94, 10.8, and 13.6 min for cyclohexene, cyclohexene oxide, 2-cyclohexen-1-ol, 2-cyclohexen-1-one, 1-octanol (internal standard), triphenylphosphine, and adipic acid, respectively). In all oxidation reactions, very little peak derived from adipic acid (TON < 0.015 with respect to Fe) was observed. Remaining hydrogen peroxide after reaction was analyzed by  $\text{Ce}^{4+}/\text{Ce}^{3+}$  titration.

## 3. Results and discussion

### 3.1. Characterization of $[\text{Fe}(\text{bpy})_3]^{2+}@\text{Y}$

ICP-AES and elemental analysis of  $[\text{Fe}(\text{bpy})_3]^{2+}@\text{Y}$  were carried out after the sample was dissolved into HF solution (Table 1).  $[\text{Fe}(\text{bpy})_3]^{2+}@\text{Y}$  sample contains 0.88 wt% iron(II) ions, 5.12 wt% C atoms, and 1.22 wt% N atoms. This result indicates that the bpy/Fe ratio is ca. 3, suggesting that Fe ion in zeolite Y was coordinated with three bpy ligands to yield  $[\text{Fe}(\text{bpy})_3]^{2+}$  ion.

IR spectra of  $[\text{Fe}(\text{bpy})_3]^{2+}@\text{Y}$ ,  $[\text{Fe}(\text{bpy})_3](\text{ClO}_4)_2 + \text{Na}-\text{Y}$ , Fe-Y, and  $[\text{Fe}(\text{bpy})_3](\text{ClO}_4)_2$  are shown in Fig. 1.  $[\text{Fe}(\text{bpy})_3](\text{ClO}_4)_2$  complex showed sharp bands in the range of 1400–1600  $\text{cm}^{-1}$  (Fig. 1(d)), which can be assigned to the  $\nu(\text{C}=\text{N})$  bands of the pyridine ring in bpy [37–39]. Similar  $\nu(\text{C}=\text{N})$  bands were observed for  $[\text{Fe}(\text{bpy})_3]^{2+}@\text{Y}$  (Fig. 1(a)) and  $[\text{Fe}(\text{bpy})_3](\text{ClO}_4)_2 + \text{Na}-\text{Y}$  (Fig. 1(b)). For  $[\text{Fe}(\text{bpy})_3]^{2+}@\text{Y}$ , the IR peaks derived from  $[\text{Fe}(\text{bpy})_3]^{2+}$  complex were observed even after Soxhlet extraction, suggesting that  $[\text{Fe}(\text{bpy})_3]^{2+}$  ions were present in the supercage of zeolite Y. The

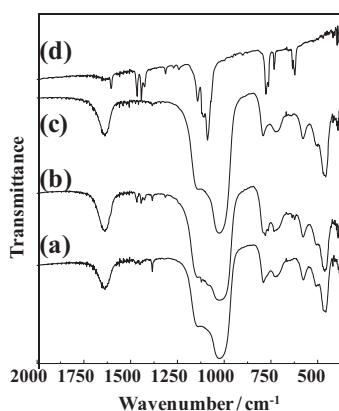


**Fig. 1.** IR spectra of (a)  $[\text{Fe}(\text{bpy})_3]^{2+}@\text{Y}$ , (b)  $[\text{Fe}(\text{bpy})_3](\text{ClO}_4)_2 + \text{Na-Y}$ , (c) Fe-Y, and (d)  $[\text{Fe}(\text{bpy})_3](\text{ClO}_4)_2$ .

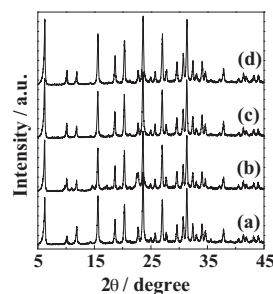


**Fig. 2.** XRD patterns of (a)  $[\text{Fe}(\text{bpy})_3]^{2+}@\text{Y}$ , (b)  $[\text{Fe}(\text{bpy})_3](\text{ClO}_4)_2 + \text{Na-Y}$ , (c) Fe-Y, and (d) Na-Y.

presence of free bpy embedded in Fe-Y was ruled out in the present study because uncomplexed bpy with smaller kinetic diameter than the pore opening of zeolite Y can be easily removed during the process of Soxhlet extraction. IR spectra of  $[\text{Fe}(\text{bpy})_3]^{2+}@\text{Y}$ ,  $[\text{Fe}(\text{bpy})_3](\text{ClO}_4)_2 + \text{Na-Y}$ , and Fe-Y showed intense bands in the range of  $1000\text{--}1200\text{ cm}^{-1}$  attributable to the  $\nu_{\text{as}}(\text{OTO})$  band, and in the range of  $700\text{--}800\text{ cm}^{-1}$  attributable to the  $\nu_{\text{s}}(\text{OTO})$  band, which are derived from zeolite framework [39,40].

XRD patterns of  $[\text{Fe}(\text{bpy})_3]^{2+}@\text{Y}$ ,  $[\text{Fe}(\text{bpy})_3](\text{ClO}_4)_2 + \text{Na-Y}$ , Fe-Y, and Na-Y were shown in Fig. 2. This figure demonstrates that the zeolite Y structure has kept even after the introduction of metal-complex. It has been reported that the empirically derived relationship between the relative peak intensities of the (220) and (311) reflections, represented by  $I_{220}$  and  $I_{311}$ , respectively, in the XRD pattern confirms the formation of a large metal complex ion in the supercage of faujasite-type zeolites:  $I_{220} > I_{311}$  for the original zeolite Y and  $I_{220} < I_{311}$  for the zeolite containing large complexes [2,30–33,41]. As can be seen in Fig. 2,  $I_{220}$  ( $2\theta = 10^\circ$ ) for physically mixed  $[\text{Fe}(\text{bpy})_3](\text{ClO}_4)_2 + \text{Na-Y}$ , Fe-Y, and Na-Y (Fig. 2(b)–(d)) was greater than  $I_{311}$  ( $2\theta = 12^\circ$ ), while the former for  $[\text{Fe}(\text{bpy})_3]^{2+}@\text{Y}$  was lower than the latter (Fig. 2(a)). These are clear evidences for the formation of complex ions within the supercage.

UV-vis diffuse reflectance spectra of  $[\text{Fe}(\text{bpy})_3]^{2+}@\text{Y}$ ,  $[\text{Fe}(\text{bpy})_3](\text{ClO}_4)_2 + \text{Na-Y}$ , Fe-Y, and Na-Y are shown in Fig. 3. No absorption was observed from the ultraviolet to visible region in the absence of metal complexes. The absorption spectrum of  $[\text{Fe}(\text{bpy})_3]^{2+}@\text{Y}$  gave four bands at 495 and 533 nm assigned to a metal-to-ligand ( $d-\pi^*$ ) charge-transfer (MLCT) [42–44], and 295 and 360 nm assigned to a  $\pi-\pi^*$  transition of the bpy ligand [44], similar to those of  $[\text{Fe}(\text{bpy})_3](\text{ClO}_4)_2 + \text{Na-Y}$  (Fig. 3(b)) and  $[\text{Fe}(\text{bpy})_3](\text{ClO}_4)_2$  in  $\text{CH}_3\text{CN}$  [45]. In spite of the same amount of  $[\text{Fe}(\text{bpy})_3]^{2+}$ , the intensity of the band assigned to  $\pi-\pi^*$  transition in  $[\text{Fe}(\text{bpy})_3]^{2+}@\text{Y}$  was larger than that in  $[\text{Fe}(\text{bpy})_3](\text{ClO}_4)_2$ .

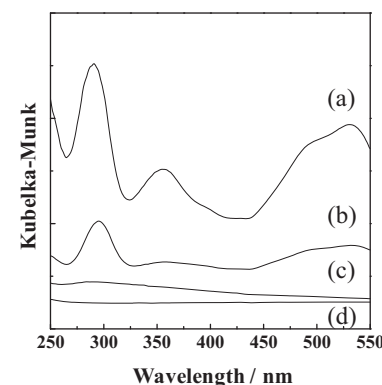


**Fig. 3.** UV-vis diffuse reflectance spectra of (a)  $[\text{Fe}(\text{bpy})_3]^{2+}@\text{Y}$ , (b)  $[\text{Fe}(\text{bpy})_3](\text{ClO}_4)_2 + \text{Na-Y}$ , (c) Fe-Y, and (d) Na-Y.

+ Na-Y. In the case of  $[\text{Fe}(\text{bpy})_3](\text{ClO}_4)_2$  single crystal (Fig. 4), the bpy ligands of  $[\text{Fe}(\text{bpy})_3]^{2+}$  are closed by  $\pi-\pi$  stacking interaction between pyridine rings of bpy ligands (C2...C9 and C3...C9': 3.576 Å, C3...C8': 3.587 Å) [46]. On the other hand, the intermolecular  $\pi-\pi$  stacking interaction of bpy ligands in  $[\text{Fe}(\text{bpy})_3]^{2+}@\text{Y}$  was inhibited by immobilization of complex into supercage [47], resulting in the increase of the intensity of the band assigned to  $\pi-\pi^*$  transition.

Fig. 5(A) shows the Fe K-edge XANES spectra of  $[\text{Fe}(\text{bpy})_3]^{2+}@\text{Y}$  together with reference compounds of  $[\text{Fe}(\text{bpy})_3](\text{ClO}_4)_2$ , Fe-Y,  $\text{Fe}_3\text{O}_4$ ,  $\text{Fe}_2\text{O}_3$  and Fe foil. The Fe K-edge XANES spectrum of  $[\text{Fe}(\text{bpy})_3]^{2+}@\text{Y}$  was quite similar to that of  $[\text{Fe}(\text{bpy})_3](\text{ClO}_4)_2$ , but was clearly different from those of other Fe-containing reference compounds of Fe-Y,  $\text{Fe}_3\text{O}_4$ ,  $\text{Fe}_2\text{O}_3$ , and Fe foil. The edge position (measured at the half-height of the edge jump) of  $[\text{Fe}(\text{bpy})_3]^{2+}@\text{Y}$  (7121.0 eV) was almost the same as that of  $[\text{Fe}(\text{bpy})_3](\text{ClO}_4)_2$  (7120.3 eV), indicating that Fe ions in both compounds have the same electronic states. FT-EXAFS spectra in Fig. 5(B) showed a strong peak at around 1.5 Å due to a Fe–N bond. The Fe–N interatomic distance of  $[\text{Fe}(\text{bpy})_3]^{2+}@\text{Y}$  was slightly shorter than that of  $[\text{Fe}(\text{bpy})_3](\text{ClO}_4)_2$ . This suggests that the encapsulated Fe(II) complexes may undergo slightly distortion or compression within supercages of Y-type zeolite due to the steric regulation induced by limited tight space.

### 3.2. Catalytic activities of Fe-containing catalysts for oxidation of cyclohexene

#### 3.2.1. Oxidation of cyclohexene with hydrogen peroxide

Que et al. [13,14] have investigated cyclohexene oxidation activities of Fe complexes with  $\text{H}_2\text{O}_2$  oxidant under the condition with 10- or 100-fold cyclohexene to  $\text{H}_2\text{O}_2$  oxidant. Such a condition that the amount of substrate is much larger than that of oxidant, is generally used in the case of re-oxidation of alcohols to ketones or aldehydes. Therefore, the similar condition was used in this report.

Fig. 6 shows the time course for oxidation of cyclohexene with  $\text{H}_2\text{O}_2$  over  $[\text{Fe}(\text{bpy})_3]^{2+}@\text{Y}$ ,  $[\text{Fe}(\text{bpy})_3](\text{ClO}_4)_2 + \text{Na-Y}$ ,  $[\text{Fe}(\text{bpy})_3](\text{ClO}_4)_2$ , and Fe-Y, under Ar. No catalytic activity for oxidation of cyclohexene with  $\text{H}_2\text{O}_2$  was observed with Na-Y and without catalyst under the same experimental condition. In the case of  $[\text{Fe}(\text{bpy})_3]^{2+}@\text{Y}$ , the amount of 2-cyclohexen-1-ol was increased with respect to time.  $[\text{Fe}(\text{bpy})_3]^{2+}@\text{Y}$  exhibited the highest yield of 2-cyclohexen-1-ol at 72 h among Fe-containing catalysts used in the present study. However, the reaction rate of  $[\text{Fe}(\text{bpy})_3]^{2+}@\text{Y}$  was much slower than those of other catalysts. This may be due to the limitation of substrate mass transfer because of small size of window (ca. 7.4 Å) for accessing to supercage of Y-type

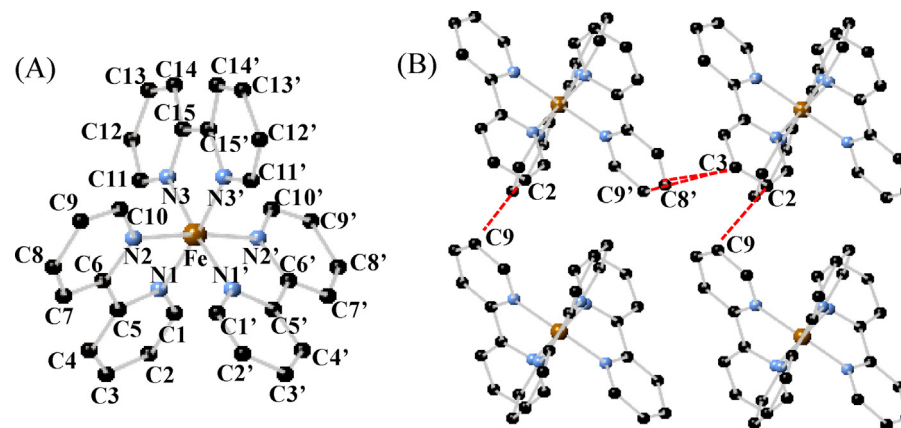


**Fig. 4.** Single crystal structure of  $[\text{Fe}(\text{bpy})_3](\text{ClO}_4)_2$ , which is viewed from 001 (A) and from 010 (B). Selected bond lengths;  $\text{Fe}-\text{N}1$ : 1.982 Å,  $\text{Fe}-\text{N}2$ : 1.978 Å,  $\text{Fe}-\text{N}3$ : 1.963 Å,  $\text{C}2-\text{C}9$ : 3.576 Å,  $\text{C}3-\text{C}9'$ : 3.576 Å,  $\text{C}3'-\text{C}8'$ : 3.578 Å.

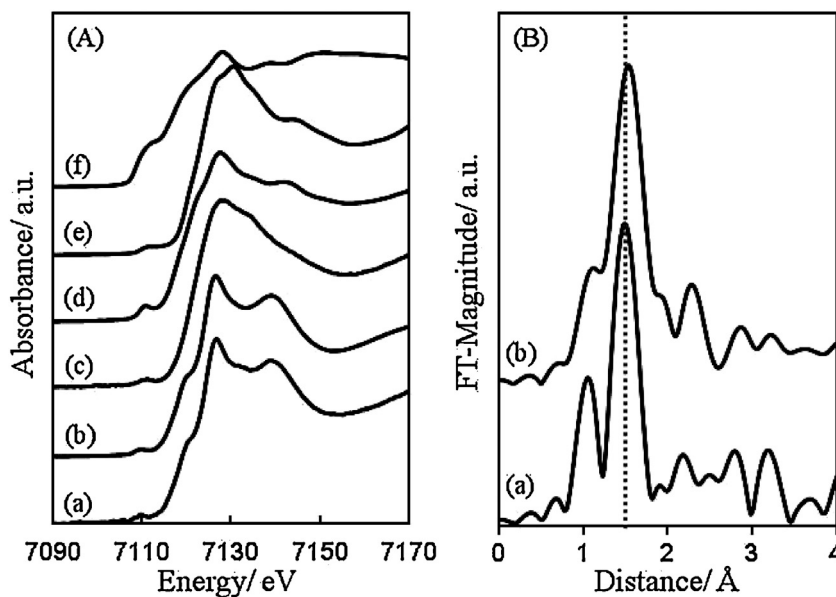


**Fig. 5.** (A) Fe K-edge XANES and (B) FT-EXAFS spectra of (a)  $[\text{Fe}(\text{bpy})_3]^{2+}@\text{Y}$ , (b)  $[\text{Fe}(\text{bpy})_3](\text{ClO}_4)_2$ , (c) Fe-Y, (d)  $\text{Fe}_3\text{O}_4$ , (e)  $\text{Fe}_2\text{O}_3$ , and (f) Fe foil.

zeolite [2,30–33], and/or due to the steric hindrance that every Fe centers in  $[\text{Fe}(\text{bpy})_3]^{2+}$  complex encounter inside the supercage.

The amounts of  $\text{H}_2\text{O}_2$  consumed after the reaction for 24 h were measured by  $\text{Ce}^{4+}/\text{Ce}^{3+}$  titration to be 0.49 mmol (61% of initial value) for  $[\text{Fe}(\text{bpy})_3]^{2+}@\text{Y}$  and 0.77 mmol (96%) for  $[\text{Fe}(\text{bpy})_3](\text{ClO}_4)_2$ . About 40% of  $\text{H}_2\text{O}_2$  still remained unreacted in the reaction solution with  $[\text{Fe}(\text{bpy})_3]^{2+}@\text{Y}$  even after 24 h reaction although the catalytic activity of  $[\text{Fe}(\text{bpy})_3]^{2+}@\text{Y}$  catalyst was higher than that of  $[\text{Fe}(\text{bpy})_3](\text{ClO}_4)_2$  catalyst. This demonstrated that the  $\text{H}_2\text{O}_2$  efficiency available for oxidation over  $[\text{Fe}(\text{bpy})_3]^{2+}@\text{Y}$  catalyst was much higher than that of  $[\text{Fe}(\text{bpy})_3](\text{ClO}_4)_2$  catalyst. The slight compression of  $[\text{Fe}(\text{bpy})_3]^{2+}$  complex in the supercage of zeolite may improve  $\text{H}_2\text{O}_2$  activation on the Fe complex.

The selectivity to 2-cyclohexen-1-ol for  $[\text{Fe}(\text{bpy})_3]^{2+}@\text{Y}$ -catalyzed oxidation of cyclohexene was *ca.* 90%, which was much higher than those for  $[\text{Fe}(\text{bpy})_3](\text{ClO}_4)_2$  and  $[\text{Fe}(\text{bpy})_3](\text{ClO}_4)_2 + \text{Na}-\text{Y}$  catalysts. The selectivity to 2-cyclohexen-1-ol was high for Fe-Y catalyst.

The recycle tests by  $[\text{Fe}(\text{bpy})_3]^{2+}@\text{Y}$  in  $\text{CH}_3\text{CN}$  demonstrated no degradation in both the catalytic activity and selectivity to 2-cyclohexen-1-ol during at least three runs (Table 2; after first reaction, the catalyst was filtrated, washed with  $\text{CH}_3\text{CN}$  for three times, dried under air, and supplied to the next catalytic run).

**Table 2**

Recycle tests of catalytic activity for oxidation of cyclohexene with hydrogen peroxide over  $[\text{Fe}(\text{bpy})_3]^{2+}@\text{Y}$  in  $\text{CH}_3\text{CN}$ .

Entry	Yield of product/ $10^{-5}$ mol (selectivity/%)		
	2-Cyclohexen-1-ol	2-Cyclohexen-1-one	Cyclohexene oxide
1st run	14.5 (89.7)	1.16 (7.2)	0.51 (3.2)
2nd run	15.3 (92.1)	0.63 (3.8)	0.68 (4.1)
3rd run	22.1 (92.6)	0.70 (3.0)	1.06 (4.4)

Reaction condition: Fe in catalysts (7.9  $\mu\text{mol}$ ), cyclohexene (7.9 mmol), 30% aqueous  $\text{H}_2\text{O}_2$  (0.8 mmol),  $\text{CH}_3\text{CN}$  (10 mL), 50 °C, Ar atmosphere, 12 h. Selectivity (%) = (product [mol])/(all products [mol]) × 100.

### 3.2.2. Effect of $\text{H}_2\text{O}$ added into $\text{CH}_3\text{CN}$ solvent for oxidation of cyclohexene

Fig. 7 shows the effect of  $\text{H}_2\text{O}$  added into  $\text{CH}_3\text{CN}$  solvent on TON for  $[\text{Fe}(\text{bpy})_3]^{2+}@\text{Y}$ ,  $[\text{Fe}(\text{bpy})_3](\text{ClO}_4)_2$ , and Fe-Y catalysts. When water was added into  $\text{CH}_3\text{CN}$  solvent, the catalytic activity of  $[\text{Fe}(\text{bpy})_3](\text{ClO}_4)_2$  significantly decreased with increasing the amount of  $\text{H}_2\text{O}$  added (Fig. 7(b)), while the catalytic activity of  $[\text{Fe}(\text{bpy})_3]^{2+}@\text{Y}$  hardly decreased (Fig. 7(a)). The TON of 2-cyclohexen-1-ol over  $[\text{Fe}(\text{bpy})_3]^{2+}@\text{Y}$  in  $\text{H}_2\text{O}$  solvent ( $x = 10 \text{ mL}$ ,  $\text{CH}_3\text{CN}$  free) was about six times larger than

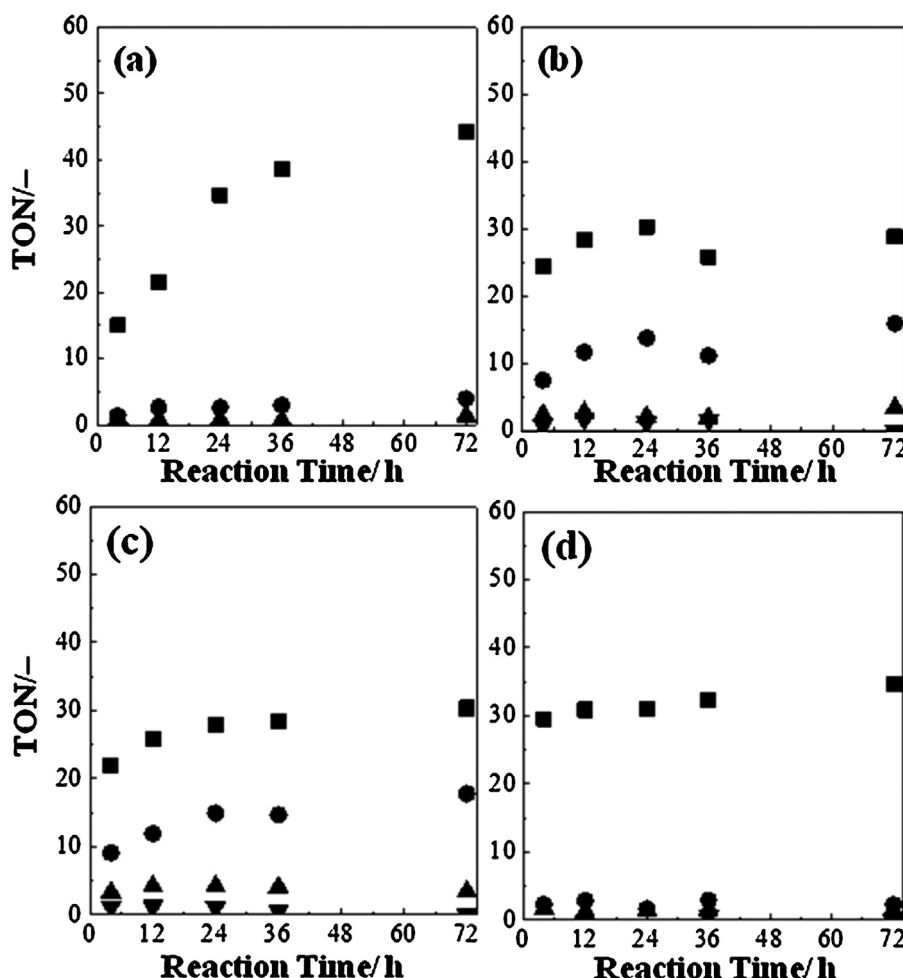


**Fig. 6.** Time course for oxidation of cyclohexene with hydrogen peroxide under Ar over (a)  $[\text{Fe}(\text{bpy})_3]^{2+}@\text{Y}$ , (b)  $[\text{Fe}(\text{bpy})_3](\text{ClO}_4)_2 + \text{Na-Y}$ , (c)  $[\text{Fe}(\text{bpy})_3](\text{ClO}_4)_2$ , and (d) Fe-Y (■; 2-cyclohexen-1-ol, ●; 2-cyclohexen-1-one, ▲; cyclohexene oxide, ▼; cyclohexan-1,2-diol). Reaction condition: Fe in catalysts (7.9  $\mu\text{mol}$ ), cyclohexene (7.9 mmol), 30% aqueous  $\text{H}_2\text{O}_2$  (0.8 mmol),  $\text{CH}_3\text{CN}$  (10 mL), 50 °C, Ar atmosphere.

that over  $[\text{Fe}(\text{bpy})_3](\text{ClO}_4)_2$  and Fe-Y catalysts, demonstrating that  $[\text{Fe}(\text{bpy})_3]^{2+}@\text{Y}$  is active and selective catalyst for oxidation of cyclohexene to 2-cyclohexene 1-ol in  $\text{H}_2\text{O}$  solvent. As mentioned previously,  $[\text{Fe}(\text{bpy})_3](\text{ClO}_4)_2$  exhibited much lower  $\text{H}_2\text{O}_2$  efficiency than  $[\text{Fe}(\text{bpy})_3]^{2+}@\text{Y}$  although it showed high  $\text{H}_2\text{O}_2$  conversion than the other Fe catalysts. The selectivity to 2-cyclohexen-1-ol on Fe-Y catalyst was similar to that on  $[\text{Fe}(\text{bpy})_3]^{2+}@\text{Y}$  catalyst; however,  $\text{H}_2\text{O}_2$  efficiency on the former catalyst was extremely lower than that on the latter catalyst. These

results suggest that the combination of  $[\text{Fe}(\text{bpy})_3]^{2+}$  and zeolite cage is indispensable for obtaining high yield of 2-cyclohexene 1-ol with high selectivity.

### 3.2.3. Oxidation of cyclohexene with molecular oxygen

Molecular oxygen ( $\text{O}_2$ ) is the most environment-friendly oxidant for oxidation of organic substrates. Therefore, the oxidation of cyclohexene with  $\text{O}_2$  instead of  $\text{H}_2\text{O}_2$  oxidant was carried out. Fig. 8 shows the time course for oxidation of cyclohexene with

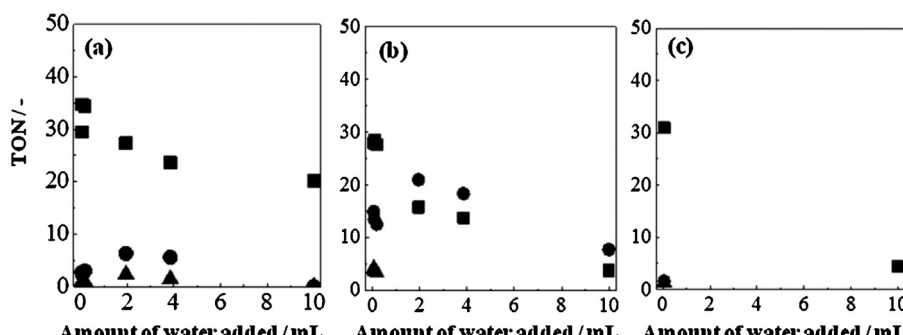


**Fig. 7.** Effect of water added into solvent on catalytic activity of (a)  $[\text{Fe}(\text{bpy})_3]^{2+}@\text{Y}$ , (b)  $[\text{Fe}(\text{bpy})_3](\text{ClO}_4)_2$ , and (c) Fe-Y (■; 2-cyclohexen-1-ol, ●; 2-cyclohexen-1-one, ▲; cyclohexene oxide, ▼; cyclohexan-1,2-diol). Reaction condition: Fe in catalysts (7.9  $\mu\text{mol}$ ), cyclohexene (7.9 mmol), 30% aqueous  $\text{H}_2\text{O}_2$  (0.8 mmol), solvent (total 10 mL;  $\text{CH}_3\text{CN}$  (10 –  $x$  mL) + water ( $x$  mL)), 50 °C, Ar atmosphere.

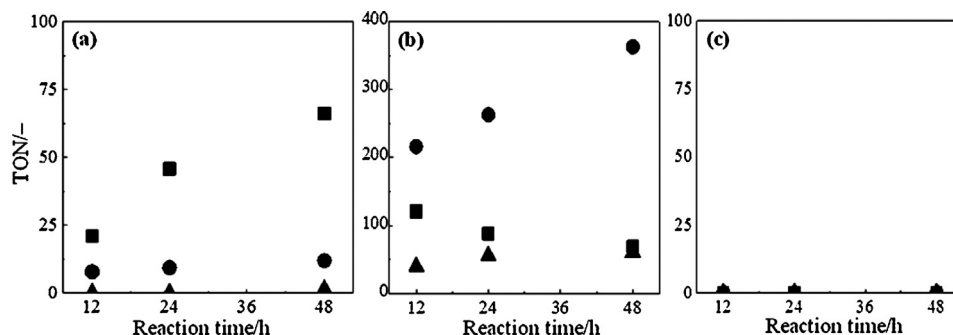
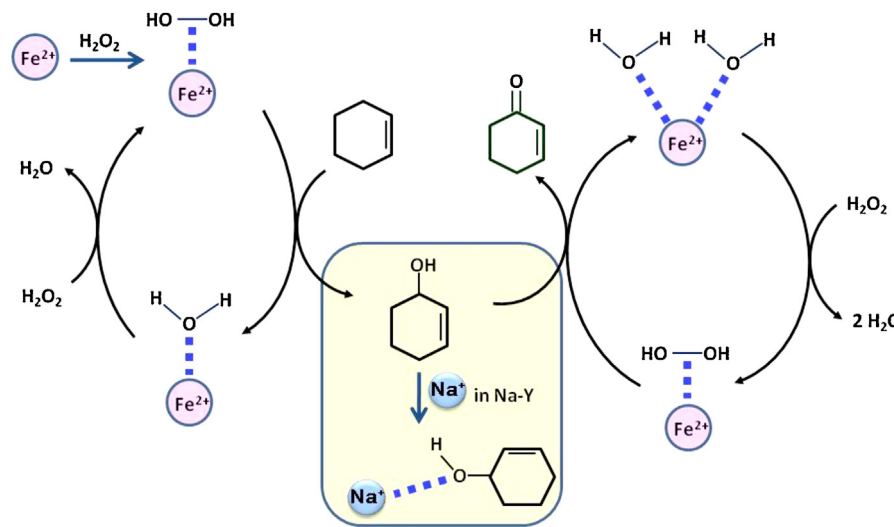


**Fig. 8.** Time course for oxidation of cyclohexene with molecular oxygen over (a)  $[\text{Fe}(\text{bpy})_3]^{2+}@\text{Y}$ , (b)  $[\text{Fe}(\text{bpy})_3](\text{ClO}_4)_2$ , and (c) Fe-Y (■; 2-cyclohexen-1-ol, ●; 2-cyclohexen-1-one, ▲; cyclohexene oxide). Reaction condition: Fe in catalysts (7.9  $\mu\text{mol}$ ), cyclohexene (7.9 mmol),  $\text{CH}_3\text{CN}$  (10 mL), 50 °C,  $\text{O}_2$  atmosphere.

(i) Homogeneous catalyst ( $[\text{Fe}(\text{bpy})_3](\text{ClO}_4)_2$ )



(ii) Heterogeneous catalysts  
 $([\text{Fe}(\text{bpy})_3]^{2+}@\text{Y}, \text{Fe-Y})$

Fig. 9. Putative mechanism for oxidation.

$\text{O}_2$  over  $[\text{Fe}(\text{bpy})_3]^{2+}@\text{Y}$ ,  $[\text{Fe}(\text{bpy})_3](\text{ClO}_4)_2$ , and Fe-Y.  $\text{CH}_3\text{CN}$  was used as a solvent because of no catalytic activity in  $\text{H}_2\text{O}$  solvent for all catalysts. In the case of  $[\text{Fe}(\text{bpy})_3]^{2+}@\text{Y}$  catalyst, the amount of 2-cyclohexen-1-ol produced was increased with respect to time. On the other hand, in the case of  $[\text{Fe}(\text{bpy})_3](\text{ClO}_4)_2$  catalyst, 2-cyclohexen-1-one was predominantly produced and its amount was increased with respect to time.  $[\text{Fe}(\text{bpy})_3]^{2+}@\text{Y}$  exhibited much higher selectivity to 2-cyclohexen-1-ol than  $[\text{Fe}(\text{bpy})_3](\text{ClO}_4)_2$ . No catalytic activity was observed for Fe-Y in the present reaction condition. This result suggests that  $[\text{Fe}(\text{bpy})_3]^{2+}$  moiety plays an important role in the present oxidation with  $\text{O}_2$  as an oxidant.

#### 3.2.4. Reaction mechanism for oxidation of cyclohexene with hydrogen peroxide

The comparison of cyclohexene oxidation in the presence and the absence of 2,6-di-*tert*-butyl-4-methylphenol as a radical-trapping reagent gave us mechanistic information. In the presence of 2,6-di-*tert*-butyl-4-methylphenol,  $[\text{Fe}(\text{bpy})_3]^{2+}@\text{Y}$  and  $[\text{Fe}(\text{bpy})_3](\text{ClO}_4)_2$  exhibited no catalytic activity. This result suggests that a radical species generated from  $[\text{Fe}(\text{bpy})_3]^{2+}$  complexes and  $\text{H}_2\text{O}_2$  plays an important role in the oxidation reaction. A putative mechanism for oxidation of cyclohexene with hydrogen peroxide is shown in Fig. 9. As can be seen in Fig. 6(b) and (c), both 2-cyclohexen-1-ol and 1-one were produced over  $[\text{Fe}(\text{bpy})_3](\text{ClO}_4)_2$

catalyst (Fig. 9(i)). On the other hand, 2-cyclohexen-1-ol was selectively generated over  $[\text{Fe}(\text{bpy})_3]^{2+}@\text{Y}$  catalyst (Fig. 9(ii)). The reaction might proceed via Fenton pathway (generation of hydroxyl radicals) due to the absence of a labile site for  $\text{H}_2\text{O}_2$  in the complex occupied by three bipyridine ligands [48–51]. Furthermore, considering that some radical species were directly observed in zeolite by ESR, the zeolite is likely to stabilize the radical species active even in water solvent [28,52–55]. The reason of such a high selectivity to 2-cyclohexene 1-ol over  $[\text{Fe}(\text{bpy})_3]^{2+}@\text{Y}$  may be due to coordination of hydroxyl group in 2-cyclohexene 1-ol to  $\text{Na}^+$  ions containing in Y-type zeolite (Fig. 9(ii)), that is, 2-cyclohexene 1-ol produced is immediately trapped by  $\text{Na}^+$  ion far from an active site,  $[\text{Fe}(\text{bpy})_3]^{2+}$ , and as a result the further oxidation of 2-cyclohexene 1-ol with  $\text{H}_2\text{O}_2$  to 2-cyclohexene 1-one hardly proceeds.

#### 4. Conclusion

Fe-bipyridine complexes encapsulated into Na-Y ( $[\text{Fe}(\text{bpy})_3]^{2+}@\text{Y}$ ) were prepared by post-ligand synthesis method to catalyze cyclohexene with  $\text{H}_2\text{O}_2$  and  $\text{O}_2$  oxidants. Several methods were performed to characterize synthesized catalyst and clarified that slightly distorted or compressed  $[\text{Fe}(\text{bpy})_3]^{2+}$  ions were formed within supercages of Y-type zeolite. The catalytic activities for oxidation of cyclohexene with  $\text{H}_2\text{O}_2$  were measured

over  $[Fe(bpy)_3]^{2+}$ @Y catalyst. The selectivity to cyclohexen-1-ol for  $[Fe(bpy)_3]^{2+}$ @Y-catalyzed oxidation of cyclohexene with  $H_2O_2$  was much higher than that for  $[Fe(bpy)_3](ClO_4)_2$  catalyst. The recovered catalyst of  $[Fe(bpy)_3]^{2+}$ @Y could be recycled at least three times without significant loss of catalytic activity and selectivity to 2-cyclohexen-1-ol. The catalytic activity depended on the amount of  $H_2O$  added into  $CH_3CN$  solvent; the catalytic activity of  $[Fe(bpy)_3]^{2+}$ @Y was hardly decreased with increasing the amount of  $H_2O$  added although that of  $[Fe(bpy)_3](ClO_4)_2$  complex was remarkably decreased. It is found that the product yield of 2-cyclohexen-1-ol over  $[Fe(bpy)_3]^{2+}$ @Y was about six times larger than those over  $[Fe(bpy)_3](ClO_4)_2$  and Fe-Y in  $H_2O$  solvent. Furthermore, it is demonstrated that the highly selective hydroxylation of cyclohexene with  $O_2$  oxidant proceeded over  $[Fe(bpy)_3]^{2+}$ @Y catalyst. The cyclohexene oxidation using a radical-trapping reagent, 2,6-di-*tert*-butyl-4-methylphenol, suggests a radical species generated from  $[Fe(bpy)_3]^{2+}$  complexes and  $H_2O_2$  plays an important role in the selective hydroxylation of cyclohexene.

## Acknowledgments

This work was supported by JSPS KAKENHI grant number 25820394. The XAFS experiments were performed at Kyushu University Beamline (SAGA-LS/BL06) with the proposal of no. 2012IK009.

## References

- [1] P.-P. Knops-Gerrits, D. De Vos, F. Thibault-Starzyk, P.A. Jacobs, *Nature* 369 (1994) 543.
- [2] D.E. De Vos, P.P. Knops-Gerrits, R.F. Parton, B.M. Weckhuysen, P.A. Jacobs, R.A. Schoonheydt, *J. Incl. Phenom. Macrocycl. Chem.* 21 (1995) 185.
- [3] F. Bediou, *Coord. Chem. Rev.* 144 (1995) 39.
- [4] M. Costas, M.P. Mehn, M.P. Jensen, L. Que Jr., *Chem. Rev.* 104 (2004) 939.
- [5] W. Nam, *Acc. Chem. Res.* 40 (2007) 522.
- [6] S.O. Kim, C.V. Sastri, M.S. Seo, J. Kim, W. Nam, *J. Am. Chem. Soc.* 127 (2005) 4178.
- [7] H. Jaafar, B. Vileno, A. Thibon, D. Mandon, *Dalton Trans.* 40 (2011) 92.
- [8] Y.-M. Lee, S. Hong, Y. Morimoto, W. Shin, S. Fukuzumi, W. Nam, *J. Am. Chem. Soc.* 132 (2010) 10668.
- [9] R. Gupta, A.S. Borovik, *J. Am. Chem. Soc.* 125 (2003) 13234.
- [10] J. Mukherjee, R.L. Lucas, M.K. Zart, D.R. Powell, V.W. Day, A.S. Borovik, *Inorg. Chem.* 47 (2008) 5780.
- [11] S. Furukawa, Y. Hitomi, T. Shishido, T. Tanaka, *Inorg. Chim. Acta* 378 (2011) 19.
- [12] Y. He, C.R. Goldsmith, *Chem. Commun.* 48 (2012) 10532.
- [13] G. Roelfes, M. Lubben, R. Hage, L. Que Jr., B.L. Feringa, *Chem. Eur. J.* 6 (2000) 2152.
- [14] K. Chen, M. Costas, J. Kim, A.K. Tipton, L. Que Jr., *J. Am. Chem. Soc.* 124 (2002) 3026.
- [15] B. Plietker, *Iron Catalysts in Organic Chemistry*, Wiley-VCH Verlag GmbH & Co. KGaA, Weinheim, 2008, pp. 1–269.
- [16] J.M. Thomas, R. Raja, D.W. Lewis, *Angew. Chem.* 117 (2005) 6614.
- [17] M. Tada, R. Couquet, J. Yoshida, M. Kinoshita, Y. Iwasawa, *Angew. Chem. Int. Ed.* 46 (2007) 7220.
- [18] K. Feng, R.Y. Zhang, L.Z. Wu, B. Tu, M.L. Peng, L.P. Zhang, D. Zhao, C.H. Tung, *J. Am. Chem. Soc.* 128 (2006) 14685.
- [19] C.-J. Li, T.-H. Chan, *Organic Reaction in Aqueous Media*, John Wiley & Sons, New York, 1997.
- [20] K. Manabe, S. Kobayashi, *Chem. Eur. J.* 8 (2002) 4094.
- [21] S. Kobayashi, C. Ogawa, *Chem. Eur. J.* 12 (2006) 5954.
- [22] C.-J. Li, *Chem. Rev.* 93 (1993) 2023.
- [23] S. Kobayashi, K. Manabe, *Acc. Chem. Res.* 35 (2002) 209.
- [24] U.M. Lindström, *Chem. Rev.* 102 (2002) 2751.
- [25] N. Aoyama, K. Manabe, S. Kobayashi, *Chem. Lett.* 33 (2004) 312.
- [26] C. Ogawa, S. Kobayashi, *Chem. Lett.* 36 (2007) 56.
- [27] T. Nagano, S. Kobayashi, *Chem. Lett.* 37 (2008) 1042.
- [28] N. Yan, C. Xiao, Y. Kou, *Coord. Chem. Rev.* 254 (2010) 1179.
- [29] Ch. Baerlocher, L.B. McCusker, D.H. Olson, *Atlas of Zeolite Framework Types*, 6th ed., Elsevier, Amsterdam, 2007.
- [30] Y. Umemura, Y. Minai, T. Tominaga, *J. Phys. Chem. B* 103 (1999) 647.
- [31] K. Mori, K. Kagohara, H. Yamashita, *J. Phys. Chem. C* 112 (2008) 2593.
- [32] R. Vijayalakshmi, S.K. Kukshreshtha, *Microporous Mesoporous Mater.* 111 (2008) 449.
- [33] W.H. Quayle, G. Peeters, G.L. De Roy, E.F. Vansant, J.H. Lunsford, *Inorg. Chem.* 21 (1982) 2226.
- [34] S. Yamaguchi, T. Fukura, C. Fujita, H. Yahiro, *Chem. Lett.* 41 (2012) 713.
- [35] H. Yahiro, T. Nagano, H. Yamaura, *Catal. Today* 126 (2007) 284.
- [36] C.-T. Lin, W. Botterher, M. Chou, C. Creutz, N. Sutin, *J. Am. Chem. Soc.* 98 (1976) 6536.
- [37] P.P. Knops-Gerrits, C.A. Trujillo, B.Z. Zhan, X.Y. Li, P. Rouxhet, P.A. Jacobs, *Top. Catal.* 3 (1996) 437.
- [38] F. Farzaneh, M. Poorkhosravani, M. Ghandi, *J. Mol. Catal.* 308 (2009) 108.
- [39] E. Holder, M.A.R. Meier, V. Marin, U.S. Schubert, *J. Polym. Sci. A* 41 (2003) 3954.
- [40] B. Hutchinson, J. Takemoto, K. Nakamoto, *J. Am. Chem. Soc.* 92 (1970) 3335.
- [41] B. Fan, W. Fan, R. Li, *J. Mol. Catal. A* 201 (2003) 137.
- [42] T.S. Morita, Y. Sasaki, K. Saito, *Bull. Chem. Soc. Jpn.* 54 (1981) 2678.
- [43] J.E. Ferguson, G.M. Harris, *J. Chem. Soc. A* (1966) 1293.
- [44] J. Fan, J. Autschbach, T. Ziegler, *Inorg. Chem.* 49 (2010) 1355.
- [45] M. Cheng, W. Ma, C. Chen, J. Yao, J. Zhao, *J. Appl. Catal. B* 65 (2006) 217.
- [46] C. Li, Z. Wu, in: S.M. Auerbach, K.A. Carrado, P.K. Dutta (Eds.), *Handbook of Zeolite Science and Technology*, Marcel Dekker, Inc., New York, 2003, pp. 423–513.
- [47] Y. Wada, T. Okubo, M. Ryo, T. Nakazawa, Y. Hasegawa, S. Yanagida, *J. Am. Chem. Soc.* 122 (2000) 8583.
- [48] Y. Mekmouche, S. Ménage, J. Pécaut, C. Lebrun, L. Reilly, V. Schuenemann, A. Trautwein, M. Fontecave, *Eur. J. Inorg. Chem.* (2004) 3163.
- [49] A.F. Trotman-Dickenson, *Adv. Free Radic. Chem.* 1 (1965) 1.
- [50] G.V. Buxton, C.L. Greenstock, W.P. Helman, A.B. Ross, *J. Phys. Chem. Ref. Data* 17 (1988) 513.
- [51] S. Miyajima, O. Simamura, *Bull. Chem. Soc. Jpn.* 48 (1975) 526.
- [52] F.L. Cozens, M. O'Neill, N.P. Scheppe, *J. Am. Chem. Soc.* 119 (1997) 7583.
- [53] W. Adam, A. Corma, M.A. Miranda, M.-J. Sabater-Picot, C. Sahin, *J. Am. Chem. Soc.* 118 (1996) 2380.
- [54] X. Liu, K.-K. Lu, J.K. Thomas, H. He, J. Klinowski, *J. Am. Chem. Soc.* 116 (1994) 11811.
- [55] B. Hwang, H. Chon, *Zeolites* 10 (1990) 101.